

# Design and Analysis of Non-Isolated DC-DC Boost Converter

Sivaraj G<sup>1</sup>, Dr Karpagavalli P<sup>2</sup>

<sup>1</sup>Sivaraj G, PhD Research scholar, Government College of Engineering, Salem, Tamilnadu, India

<sup>2</sup>Dr Karpagavalli P, Professor (CAS), Government College of Engineering, Salem, Tamilnadu, India

\*\*\*

**Abstract** - In this paper, design of Non-isolated DC-DC Boost converter using three switches is presented. The proposed converter has significant advantages such as high voltage gain, non-inverting output, low voltage stress and high efficiency. By using three switches and boosting capacitor, high conversion ratio is attained with good efficiency. Transformer or coupler inductor is not used which eliminates high voltage spikes and the need of active/passive clamping circuits. In the proposed converter, continuous conduction operation can be done easily and effectively. Three switches use two duty ratios which helps in achieving high voltage conversion without operating the switches in extreme duty cycles. This allows to operate the converter with lesser conduction losses. The detailed operation of the introduced converter is discussed and presented. Simulation is done in both open and closed loop configuration of the converter to verify the performance of the proposed DC-DC Boost converter.

**Key Words:** Boost Converter, boosting capacitor, three switches

## 1. INTRODUCTION

Renewable energy gains the attention in the recent decades because of clean power generation. DC-DC converter become one of the important component for voltage conversion from one voltage level to other [1,2]. In recent past conventional DC-DC boost converter is used for high voltage conversion. However voltage stress on switch is equal to voltage output. Hence higher rated switch is chosen to meet voltage stress which results in higher conduction loss. In addition, large duty ratio for high voltage gain causes higher conduction loss and high spike voltages.

Various isolated dc-dc converter configurations are proposed in literature to achieve high conversion ratio [3-6]. However challenges associated with this type of converter is saturation in the transformer core. Hence non-isolated dc-dc converters can be used to attain high voltage gain with compact size and reduced cost. Some non-isolated high gain converters are cascade boost[7], quad boost and switched capacitor converters. The inclusion of switched capacitor or inductor adds the cost and complexity.

Various coupled inductor based boost converters provide high voltage conversion and low volt stress on switch based on duty ratio selection [9-11]. Sometimes increase in turns ratio of coupled inductor for high voltage gain, results in high

current ripples. Hence, input filter is needed to reduce current ripple[12].

In this paper, novel high gain non-isolated DC-DC boost converter is proposed to overcome above mentioned issues. The proposed converter has high voltage gain by operating three switches in two different duty ratios. Since the two different duty ratios can be used, conduction losses can be reduced by not operating the switches in extreme duty ratios and in addition, clamping circuits are not needed to address high voltage spike issues. It has reduced voltage stress on switches and diodes.

The circuit description and steady state analysis of converter is presented in section II and III. Section IV explains the simulation result and discussion. Conclusion is presented in Section V.

## 2. PROPOSED HIGH GAIN TOPOLOGY

The proposed converter is shown in Fig 1. Which consists of three power semiconductor switches  $M_1$ ,  $M_2$  and  $M_3$ , two capacitors  $C_a$  and  $C_o$ , two inductors  $L_m$ ,  $L_n$  and three diodes  $D_a$ ,  $D_s$ ,  $D_o$ . The switches operate with switching frequency  $f_s$ .  $D_1$  is the duty ratio of MOSFET switches  $M_1$  and  $M_2$ .  $D_2$  is the duty ratio of  $M_3$ .

In order to explain steady state operation, some following assumptions are made.

- (i) All components in the converter circuit are ideal
- (ii) The effects of ON-state resistances of switches, equivalent series resistance (ESR) of inductors and capacitors and forward voltage drops of diodes are neglected.
- (iii) Output capacitance is large enough to maintain output voltage  $V_o$ .
- (iv) Number of turns of inductors are equal so that  $L_m = L_n = L$ .

## 3. MODES OF OPERATION

Based on aforementioned assumptions, Modes of operation can be subdivided into three modes in Continuous conduction mode (CCM) operation. Switch ON operation covers first two modes and switch OFF operation will be in third mode. The detailed operation is discussed in this section.

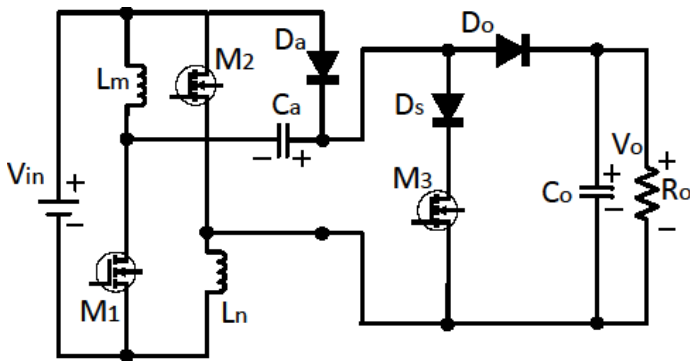


Fig -1: Proposed DC-DC Boost converter

### 3.1 Mode I

During the time interval [to to t1], simultaneously MOSFETs M1 and M2 are turned ON and MOSFET M3 is turned OFF. Current flow path is depicted in Fig. 2(a). The energy is fed from source voltage to inductors Lm and Ln and capacitor Ca through diode Da. Simultaneously stored energy in output capacitor Co is discharged to load resistor Ro. Meanwhile diodes Ds and Do are in reverse biased condition. In this mode, capacitors Ca and inductors Lm and Ln are parallel to source, therefore voltage across them are as given in equations [1].

$$V_{Lm} = V_{Ln} = V_{Ca} = V_{in} \quad (1)$$

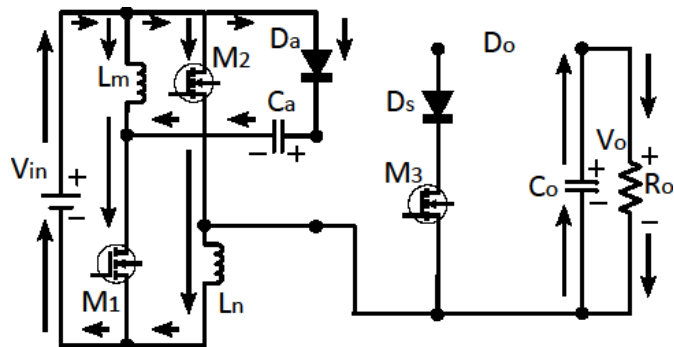


Fig -2(a): Mode I operation

### 3.2 Mode II

During time interval [t1 to t2], MOSFETs M1 and M2 are simultaneously turned OFF and MOSFET M3 is made ON. The current flow path is shown in Fig. 2(b). The energy is fed from source to capacitors and inductors through the path Lm, Ca, Ds and Ln. In this mode, voltage across MOSFETs M1 and M2 is half of Input source voltage. Since Do is reverse biased, output capacitor Co still discharges the stored energy to the load resistor Ro. Inductors Lm, Ln and capacitor Ca are in series connection to the source voltage and the voltage across them are given as in equations [2] and [3].

$$V_{Lm} - V_{Ca} - V_{Ln} = V_{in} \quad (2)$$

$$2V_L = V_{in} + V_C \quad (3)$$

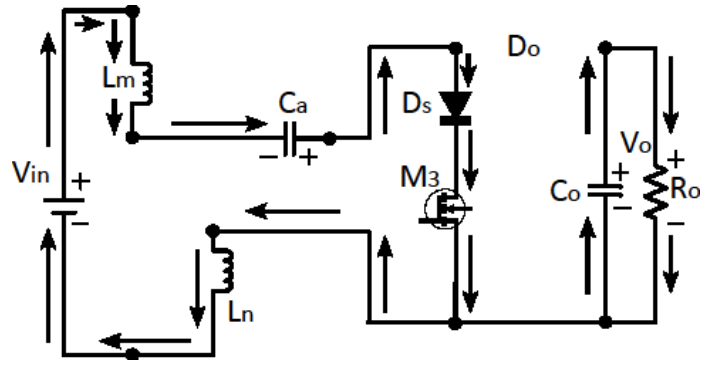


Fig -2(b): Mode II operation

### 3.3 Mode III

During the interval [t2 to t3], all the power semiconductor switches M1, M2 and M3 are turned OFF. The current flow path is shown in Fig. 2(c). In this mode, source and stored energy from inductors and capacitors supply the load resistor Ro. Diode Da and Ds are in reverse biased condition. Do is forward biased, therefore output capacitor Co is charged during this mode. In this mode, inductors Lm, Ln and capacitors Ca are in series to source and load. The voltage across inductors Lm and Ln are as given in equations [4].

$$V_{Lm} + V_{Ln} = 2V_L = V_{in} + V_C - V_o \quad (4)$$

Where Vo is voltage output of proposed converter.

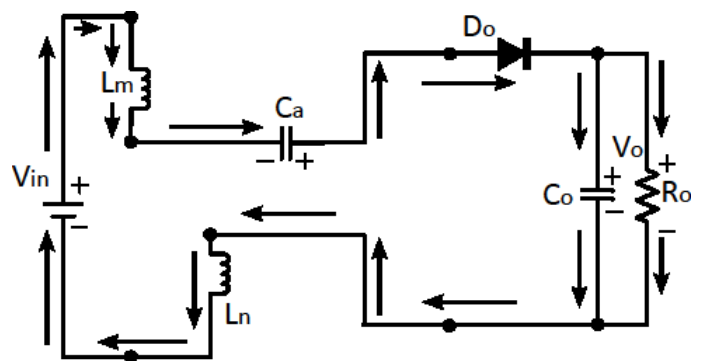


Fig -2(c): Mode III operation

The ideal voltage gain of the converter can be determined as in equation [5].

$$V_o/V_{in} = 2/(1-D_1-D_2) \quad (5)$$

From the above equation it is observed that two duty ratios shall not be equal and the sum of the two duty ratios shall not be greater than unity.

Similarly neglecting ESR of capacitors, inductors, diodes and switches, current gain can be computed as follows in equation (6).

$$I_{in}/I_o = 2/(1-D_1-D_2) \quad (6)$$

### 3.4 Mode IV (DCM OPERATION)

The proposed converter operates in DCM if current in the inductor reduces to zero during switching OFF interval. Hence DCM operation has four modes of operation. Mode I, II and III are same as that of CCM operation. Whereas in Mode 4 switches  $M_1$ ,  $M_2$  and  $M_3$  and the diodes  $D1$  and  $D2$  are turned OFF and voltage across inductors are approximately equal to zero.

### 4. SIMULATION RESULTS AND DISCUSSION

For the simulation, values of the capacitors  $C_a$  used is 5uF. The output Capacitor  $C_o$  is chosen as 20uF. The switching frequency of the MOSFET is 40kHz with two duty cycles 50% for  $M_1$  and  $M_2$  switches and 35% for  $M_3$  switch. All parameter values used in simulation are shown in Table - 1. Open loop and closed loop topology for the proposed converter is depicted in Fig. 3(a) and Fig. 3(b) respectively. The comparison is done between open loop and closed loop of proposed converter in simulation environment. In open loop circuit, input voltage is 30V and obtained output voltage is 389V. In closed loop PI circuit, for the same input voltage, obtained voltage output is 397V. The ripple voltage is 1.5V in open loop and less than 1V in closed loop which is better. Fig.4 shows the switching gate pulse VG for MOSFET's  $M_1$ ,  $M_2$  and  $M_3$ .

**Table -1:** Simulation parameters of proposed converter

Circuit parameters	Symbol	Values
Input voltage	$V_{in}$	30V
Output voltage	$V_o$	400V
Load resistor	$R_L$	533 ohms
Switching frequency	$f_s$	40kHz
Inductors	$L_m$ and $L_n$	200uH
Capacitor	$C_a$	5uF
Output capacitor	$C_o$	20uF

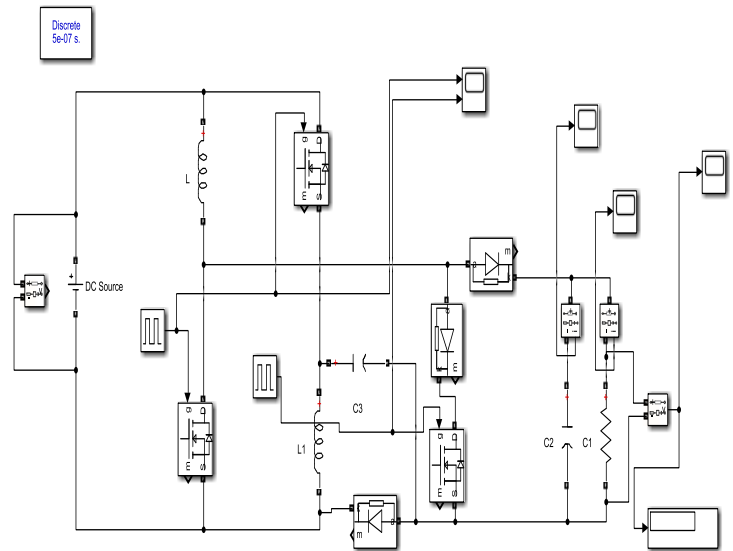


**Fig -3(a):** Simulation diagram of Proposed converter – Open loop model

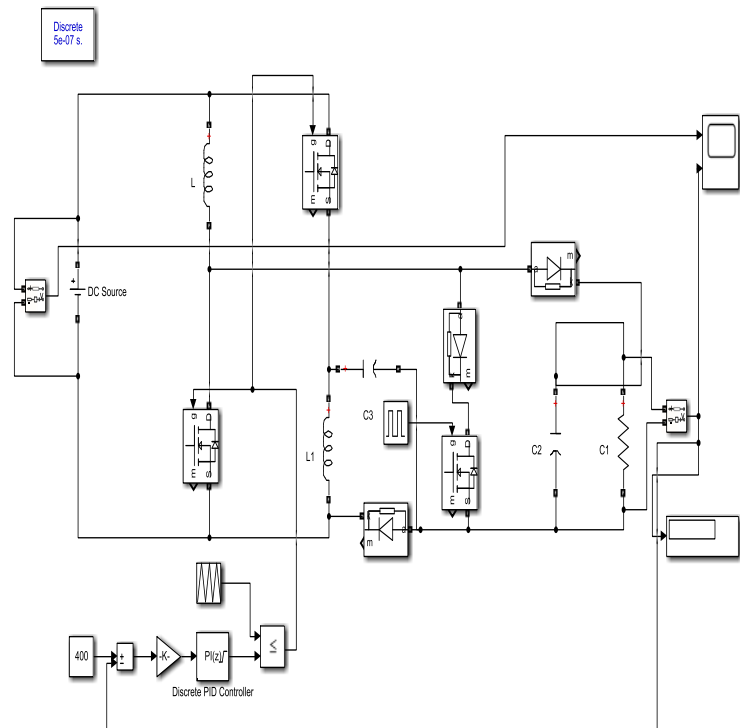


**Fig -3(b):** Simulation diagram of Proposed converter – Closed loop model

The output waveforms of the voltage  $V_o$  in open loop and closed loop are shown in Fig. 5a and 5b respectively. It is observed that voltage gain of 13.33 with ripple of 1V is obtained for the input of 30V in closed loop and ripple of 1.5V is obtained in open loop.

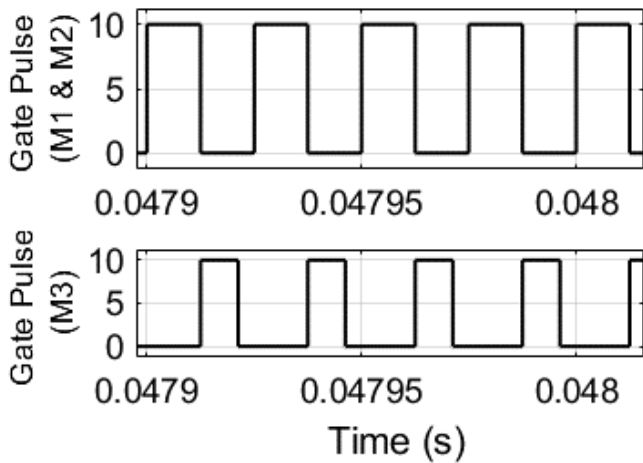


Fig-4: Gate pulse of MOSFETs M<sub>1</sub>, M<sub>2</sub> and M<sub>3</sub> for the proposed converter

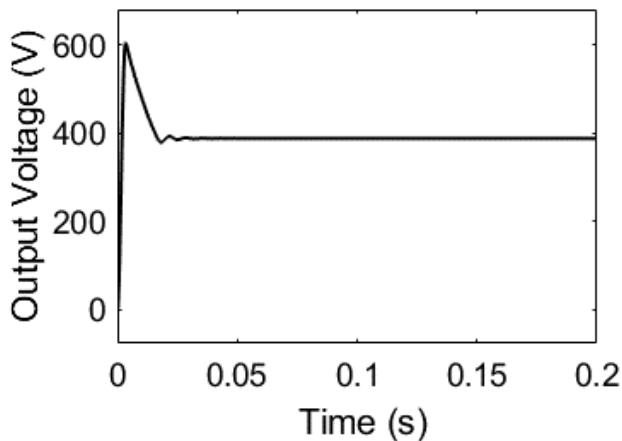


Fig-5(a): Output Voltage waveform of the Proposed converter in Open loop config.

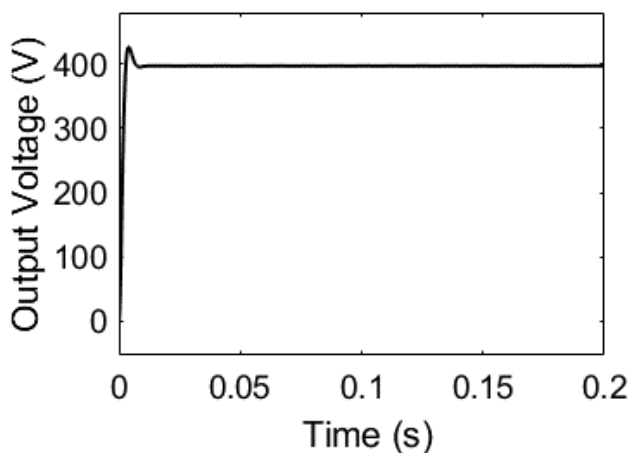


Fig-5(a): Output Voltage of Proposed closed loop topology

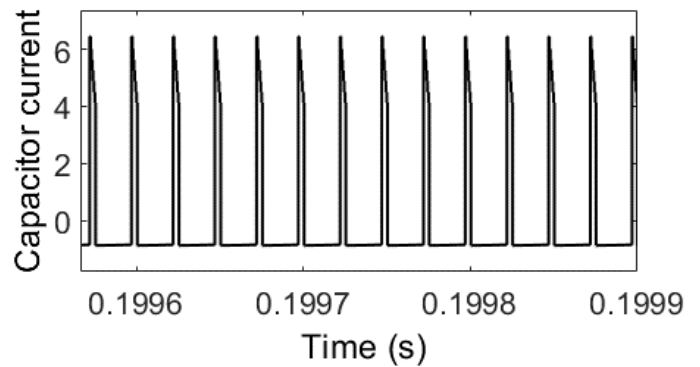


Fig-6: Capacitor current of the Proposed converter.

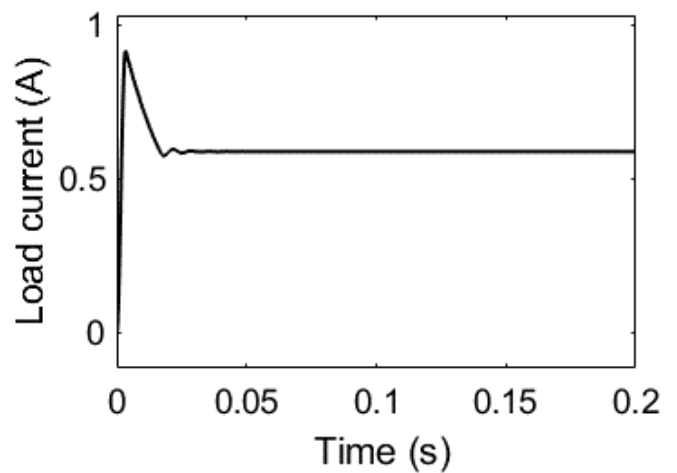


Fig-7(a): Output current waveform of the Proposed converter in open loop config.

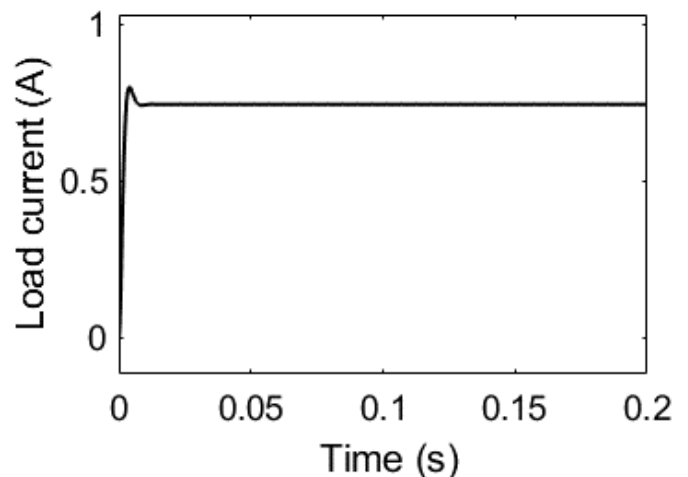


Fig-7(b): Output current waveform of the Proposed converter in closed loop config

Peak overshoot voltage is more in open loop structure compared to closed loop structure. For an output voltage of 400V, peak overshoot of 600V is obtained in open loop circuit. Whereas in closed loop topology, peak overshoot of 425V is obtained which is very much lesser and acceptable. Input current is the sum of input inductor currents which are

same and continuous and their slopes are increasing. Fig. 6 shows the waveform of capacitor current  $I_c$  and it is observed that capacitor is charged during OFF mode. Output voltage closer to the theoretical gain is obtained in closed loop topology.

The output waveforms of the load current  $I_o$  in open loop and closed loop are shown in Fig. 7a and 7b respectively. It is inferred that for input current of 10A, average value of output current is 690mA and 740mA in open loop and closed loop respectively. Closed loop delivers more current. Thus closed loop enhances the output voltage, current, ripple voltage and efficiency.

**Table -1:** Comparison tabulation of Proposed converter in Open loop and Closed loop configuration

Proposed Converter parameters	Source voltage/Input voltage (V)	Output voltage (V)
Theoretical voltage value	30V	400V
Simulation value in open loop structure	30V	389V
Simulation value in closed loop structure	30V	397V

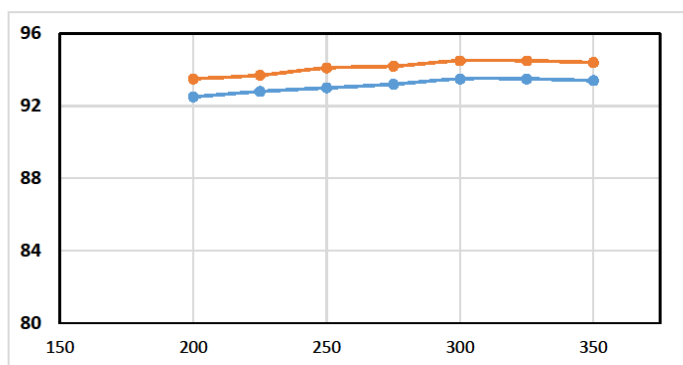


**Fig -8:** Comparison of Efficiency in open loop and closed loop control of the proposed converter

Inorder to verify performance of proposed non-isolated boost converter, prototype of 300W has been developed in the laboratory. Component parameters of the prototype are as shown in Table 1. The performance comparison between open loop and closed loop topology of proposed converter is shown in Table 2. Considering closed loop structure of the proposed converter, its waveforms of the converter while operating in CCM at 40kHz switching frequency with  $D_1 = 50\%$  and  $D_2 = 35\%$  duty ratio, Voltage gain is approximately 13.33 and output voltage is 397V. The output voltage ripple with output capacitor is less than 1.5V which is very well

acceptable. The output current is 720mS which indicates that output power obtained is 300W.

Eventually, power efficiency curve for the proposed converter is depicted and compared with open and closed loop structure in Fig. 8. Closed loop structure achieved higher efficiency when compared with open loop configuration.

## 5. CONCLUSION

A new high gain non-isolated DC-DC boost converter has been presented in detail. The principle of operation, voltage gain analysis and simulation results and discussion is presented in detail. DC-DC converter accomplishes high voltage gain of 13.33 to produce an output of 400V by operating three switches with two duty cycle and thus offering wide operating range which is unique in this converter. DC-DC converter offers high voltage compared with lesser peak overshoot in closed loop configuration as compared to open loop topology. Moreover high voltage gain is achieved without using coupled inductors. Therefore no voltage overshoot across switches and no clamping circuit is needed and thus compact size is achieved. This effect reduces conduction losses in the proposed converter and thus offers better efficiency. Finally simulated results and efficiency comparison were presented to validate the advantages of proposed high voltage gain converter.

## REFERENCES

- [1] N. Eghtedarpour and E. Farjah, "Distributed charge/discharge control of energy storages in a renewable-energy-based DC micro-grid," *IET Renew. Power Gen.*, vol. 8, no. 1, pp. 45-57, January 2014.
- [2] M. Carrasco et al., "Power-Electronic Systems for the Grid Integration of Renewable Energy Sources: A Survey," *IEEE Trans. Ind. Electron.*, vol. 53, no. 4, pp. 1002-1016, June 2006.
- [3] Padmanabhan, S., Bhaskar, M., Maroti, P., et al.: 'An original transformer and switched-capacitor (T & SC)-based extension for DC-DC boost converter for high-voltage/low-current renewable energy applications: hardware implementation of a new T & SC boost converter', *Energies*, 2018, 11, (4), p.783
- [4] Nehrir, M.H., Wang, C., Strunz, K., et al.: 'A review of hybrid renewable/alternative energy systems for electric power generation: configurations, control, and applications', *IEEE Trans. Sustain. Energy*, 2011, 2, (4), pp. 392- 403
- [5] Das, M., Agarwal, V.: 'Novel high-performance stand-alone solar PV system with high-gain high-efficiency DC-DC converter power stages', *IEEE Trans. Ind. Appl.*, 2015, 51, (6), pp. 4718-4728
- [6] F. L. Tofoli, D. d. C. Pereira, W. Josias de Paula and D. d. S. Oliveira Júnior, "Survey on non-isolated high-voltage step-up dc-dc topologies based on the boost converter," *IET Power Electron.*, vol. 8, no. 10, pp. 2044-2057, Oct. 2015.

- [7] [Yang, J., He, Z., Pang, H., et al.: 'The hybrid-cascaded DC-DC converters suitable for HVDC applications', IEEE Trans. Power Electron., 2015, **30**,(10), pp. 5358-5363
- [8] B. Bryant and M. K. Kazimierczuk, "Voltage-Loop Power-Stage Transfer Functions With MOSFET Delay for Boost PWM Converter Operating in CCM IEEE Trans. Ind. Electron., vol. 54, no. 1, pp. 347- 353, Feb. 2007.
- [9] Forouzesh, M., Shen, Y., Yari, K., et al.: 'High-efficiency high step-up DC-DC converter with dual coupled inductors for grid-connected photovoltaic systems', IEEE Trans. Power Electron., 2018, **33**, (7), pp. 5967-5982
- [10] Siwakoti, Y.P., Mohsen, S., Blaabjerg, F., et al.: 'High voltage gain quasi-SEPIC DC-DC converter', IEEE J. Emerg. Sel. Top. Power Electron., 2018,**7**, (2), pp. 1243-1257, DOI: 10.1109/JESTPE.2018.2859425
- [11] Sagar Bhaskar, M., Meraj, M., Iqbal, A., et al.: 'High gain transformer-less Double-duty-triple-mode DC/DC converter for DC microgrid', IEEE Access, 2019, 7, pp. 36353-36370
- [12] X. Wu, J. Zhang, X. Ye and Z. Qian, "Analysis and Derivations for a Family ZVS Converter Based on a New Active Clamp ZVS Cell," IEEE Trans. Ind. Electron., vol. 55, no. 2, pp. 773-781, Feb. 2008.
- [13] Ardi, H., Ajami, A.: 'Study on a high voltage gain SEPIC-based DC-DC converter with continuous input current for sustainable energy applications', IEEE Trans. Power Electron., 2018, **33**, (12), pp. 10403-10409
- [14] Xia, Y., Wei, W., Yu, M., et al.: 'Power management for a hybrid AC/DC microgrid with multiple subgrids', IEEE Trans. Power Electron., 2018, **33**, (4), pp. 3520-3533
- [15] Sathyan, S., Suryawanshi, H.M., Shitole, A.B., et al.: 'Soft-switched interleaved DC/DC converter as front-end of multi-inverter structure for micro grid applications', IEEE Trans. Power Electron., 2018, **33**, (9), pp. 7645-7655
- [16] BaDawy, M.O., Husain, T., Sozer, Y., et al.: 'Integrated control of an IPM motor drive and a novel hybrid energy storage system for electric vehicles', IEEE Trans. Ind. Appl., 2017, **53**, (6), pp. 5810-5819
- [17] Jyotheeswara Reddy, K., Sudhakar, N.: 'High voltage gain interleaved boost converter with neural network based MPPT controller for fuel cell based electric vehicle applications', IEEE Access, 2018, **6**, pp. 3899-3908
- [18] Haimin, T., Duarte, J.L., Hendrix, M.A.M.: 'Line-interactive UPS using a fuel cell as the primary source', IEEE Trans. Ind. Electron., 2008, **55**, (8), pp.3012-3021
- [19] Nymand, M., Andersen, M.A.E.: 'High-efficiency isolated boost DC-DC converter for high-power low-voltage fuel-cell applications', IEEE Trans. Ind. Electron., 2010, **57**, (2), pp. 505-514
- [20] Hwu, K.I., Jiang, W.Z.: 'Isolated step-up converter based on flyback converter and charge pumps', IET Power Electron., 2014, **7**, (9), pp. 2250-2257